Milling Dynamics: Part I. Attritor Dynamics: Results of a Cinematographic Study

R.W. RYDIN, D. MAURICE, and T.H. COURTNEY

The motions of grinding media and powder in an attritor canister were studied by means of filming the agitated charge and frame-by-frame scrutiny of the footage. In conjunction with auxiliary experiments, this permitted semiquantitative analysis of the milling action. In particular, the mill can be divided into several regions characterized by different balances between direct impacts and rolling/sliding of the grinding media. Simple calculations suggest that impacts are more capable of effecting mechanical alloying (MA) than are rolling or sliding events in an attritor. Powder circulation within an operating mill was also investigated. Based on the results and the accompanying analysis, concepts for improved attritor design are presented.

I. INTRODUCTION

MECHANICAL alloying (MA) is a technique for producing powders manifesting intriguing properties. Originally developed by Benjamin and co-workers[1] some 20 years ago, MA may be described as the repeated deformation, fracture, and welding of powder by a highly energetic ball charge.[2,3] Initial applications of MA focused on the production of oxide dispersion-strengthened superalloys,[4,5] now commercially available. More recently, Al-based powders having structural uses have been developed.[6,7] Within the last decade or so, the use of MA has been extended, at least on a laboratory scale, to the production of other kinds of materials. Intermetallics,[8,9] inorganic nonmetallics,[10,11] nonequilibrium phases and structures,[12,13] nanocrystals,[14,15] and amorphous materials[16,17] can all be synthesized by MA.

Mechanical alloying can be conducted in a variety of devices. Commercial production is carried out in large ball or rod mills (approximately 2 m in diameter) having significant capacities. As a result of the low-energy densities of these mills, production times are long, on the order of a week. Higher energy mills require less time to "alloy" but also have lesser capacities. For example, an attritor is a common laboratory device used for MA; larger sized attritors are also feasible for small-scale commercial production. Times required to "alloy" in an attritor are typically much less than they are with large commercial mills. Still higher energy mills, such as the shaker mill (exemplified by a SPEX mill) and the planetary mill, require even lesser times for process completion. Higher energy mills are the ones usually used to produce nonequilibrium manifestations (*e.g.*, amorphous materials) of MA.

Some aspects of what occurs during MA have been known qualitatively for some time.[2,3] But description of the MA process is complex and multifaceted, as it involves concepts of mechanics, mechanical behavior, heat flow, thermodynamics, and kinetics. In spite of (perhaps because of) this, modeling of MA has been an avenue of recent interest.[18–25] Modeling approaches can be classified into two types, local and global. Local modeling describes the various effects (thermal and mechanical) and events (deformation, fracture, and welding) that transpire when powder particles are entrapped between two colliding or sliding surfaces.[18–20,22] Thus, local modeling is generic in the sense that parameters (relative impact velocity, angle of impact between colliding workpieces, charge ratio, *etc.*) affecting the various events are common to all devices, although the values of some of the parameters (*e.g.*, relative impact velocity) are specific to a particular type of mill and its operating conditions. Global modeling is device specific. For example, this type of modeling entails the study of factors such as the distribution of impact angles and the heterogeneity of powder distribution within the mill,[21,23–25] factors which clearly differ from one type of device to another. Successful modeling of MA depends upon effective synthesis of the local and global approaches.

In this article, we describe the global dynamics of an attritor. The description is based on observations made through high-speed filming of a mill in action. The resulting video record was combined with measurements of ball velocities within different regions of the attritor and with results of ancillary experiments. This study allowed us to partition the attritor into volumes where different processes (*e.g.*, rolling/sliding, impacts) occur at different rates. Based on the results of this work, several suggestions for improved attritor design are offered. In Part II of this series, we will compare the dynamics of the attritor to that of a SPEX mill and explore how the differences between them affect the properties and dimensions of the product powder.

II. PREVIOUS STUDIES

In the following paragraphs, previous attempts at modeling attritor dynamics are reviewed. Conclusions therefrom are discussed in light of results obtained from the present work, which are elaborated on subsequently.

The complexity of past modeling has ranged from simple physical observations to erudite mathematical treatises. An example of the former can be found in attritor modeling using a fluid mechanics approach.[18,24] This

R.W. RYDIN, Graduate Student, is with the Materials Science Program, University of Delaware, Newark, DE 19716. D. MAURICE is formerly a Graduate Student, Department of Materials Science and Engineering, University of Virginia, Charlottesville, VA 22903. T.H. COURTNEY, Professor and Chair, is with the Department of Metallurgical and Materials Engineering, Michigan Technological University, Houghton, MI 49931.

Manuscript submitted July 20, 1992.

approach has been encouraged by the observation that balls located at the attritor periphery are displaced vertically with respect to those in the attritor interior. The relative displacement, and its dependence on attritor angular velocity, can be mimicked by treating the attritor ball charge as a viscous fluid. Lavarev *et al.*[24] attempted to model attritor milling using a finite element approach, assuming also that the balls behave like a fluid. They presumed (correctly, as we shall see) that the attritor arms transmit the driving force to the ball charge along relatively narrow horizontal zones and that the balls outside these zones attain their velocity by transmission of impulses from balls within the zones. However, Lavarev *et al.* failed to identify the forms of the various mechanical actions (*e.g.*, ball impacts *vs* ball sliding). A more serious criticism is that when applied to a laboratory-sized attritor (and likely to a commercial unit as well), the mesh size used for their finite element program is smaller than the size of typical grinding media. Thus, they predicted velocity profiles which do not take into account the discrete character of the grinding media.

The "mechanical actions" alluded to above are responsible for the fracture and coalescence mechanisms of MA. These have been described in a generic (local) sense in a number of articles. Global descriptions of them for an attritor can be couched in principles of comminution taking place in ball and/or rod mills. For example, Rose and Sullivan[26] identify three distinct mechanisms involved in the size reduction of ores. The first is direct crushing, commonly associated with an impact event. The second is shearing or abrasion among particles in the feed trapped between the grinding media; this is similar to rolling/sliding between balls in an attritor. The third mechanism identified by Rose and Sullivan is shearing and abrasion between the mill lining and the media. In this article, we show that the second mechanism is likely of little import for MA in an attritor and that the first and third mechanisms are more dominant in certain regions of an attritor than others.

A more recent description of attritor milling is due to Goodson *et al.*[25] They suggest that processed material is trapped between balls, and the material is subject to a combination of rubbing and impingement between balls, between balls and the impeller shaft, and to a much lesser extent, between balls and the chamber walls. Goodson *et al.* present a hypothetical radial velocity profile, as shown in Figure 1. We will show that the form of this profile is correct in general, but that there are nuances which can only be determined empirically. Further, we note that the two-dimensional description given by Goodson *et al.* does not adequately portray the three-dimensional global dynamics of an attritor.

Kimura *et al.*[27] considered energy input as affecting the mechanical and geometrical aspects of attritor milling. They reported that agitator arm torque is proportional to the rotational speed raised to a power greater than unity. It was speculated that the increased torque required at higher revolutions per minute (rpm) was due to the ball array, as well as the motion of individual balls, becoming more random with increasing rotational speeds. Contrary to this, we observe an increased tendency toward collective motion of the grinding media, as well as a tendency for the balls outside of the impeller region to assume a close-packed array, with increased rotational frequency.

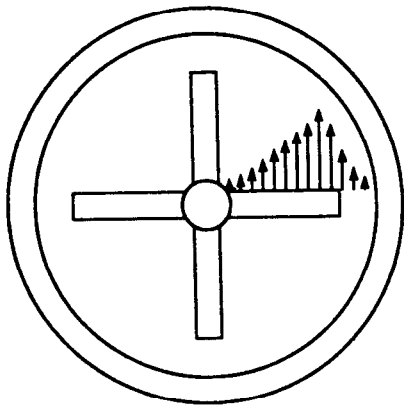

Fig. 1—Radial ball velocity profile in an operating attritor, as proposed by Goodson *et al.*[25]

We are unaware of any previous efforts to investigate powder circulation within the mill. In this study, we demonstrate the heterogeneous distribution of powder within an attritor and, based on dynamical observations of the device, suggest plausible mechanisms for powder circulation within the mill.

III. DESCRIPTION OF THE CINEMATOGRAPHIC TECHNIQUE

A custom attritor (Figure 2) was used for media motion studies. Several adaptive changes were necessary in the traditional design in order for us to carry out our objectives of identifying the rolling and impact zones and tracing powder migration during milling. A clear PLEXIGLAS* tank was incorporated, rendering the grinding media visible for filming. A microsecond timer and a tachometer were built into the attritor control loop (Figure 2), enabling us to determine both impeller and media velocities. Finally, the mill container and drive motor were secured to a bar permitting 180 deg of rotation so that we could rotate the mill and have an unobstructed view of the top and bottom of the ball charge.

*PLEXIGLAS is a trademark of Rohm & Haas Company, Philadelphia, PA.

Although we observed mill behavior over a continuous range of rotational speeds from 0 to 550 rpm, actual filming was carried out at 50 and 250 rpm. These speeds were chosen because they illustrate the two distinct modes of ball packing (disordered and close-packed) observed along the container wall. Attritors of the type we studied are often operated at the higher rotational velocities (*e.g.*, 550 rpm). However, the film and frame speeds used in this study were not sufficiently fast to resolve events taking place at these velocities. Illumination of the attritor with stroboscopic lighting at an operational frequency of 550 rpm, though, indicated little qualitative difference between attritor dynamics at 250 and 550 rpm.

The resulting video recordings, along with related observations, allowed us to ascertain velocities (and velocity gradients) in different regions of the mill. Since

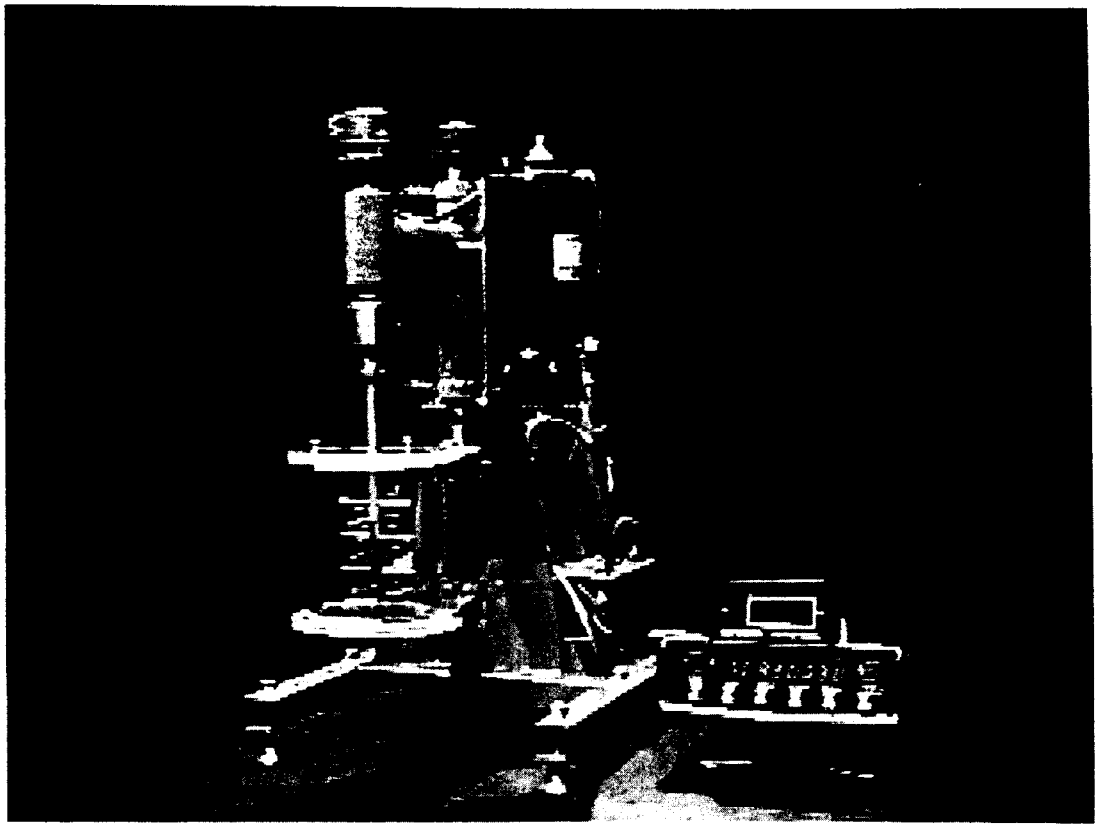

Fig. 2—Photograph of custom attritor. The transparent tank permits viewing of media and powder motion. The microsecond timer and tachometer (to the right of the attritor) enable impeller and media velocities to be determined.

the mill contained stainless steel balls, observations were necessarily confined to the wall surfaces and to the top and bottom parts of the canister.

Powder migration during milling was also studied in order to determine the powder distribution and migration pattern. To this end, a highly visible powder, which contrasted with the grinding media and whose particle size was similar to that of typical mechanically alloyed powders, was required. We chose DRIERITE* ($CaSO_4$) and ground it with a mortar and pestle to approximately −100 mesh. Residual moisture was baked out prior to use to avoid undesirable powder clumping.

*DRIERITE is a trademark of Drierite Company, Xenia, OH.

A number of "still shots" taken from the video recordings are presented in this article. These are used for illustrative purposes, and several of them do not reflect the clarity evident in the original film. However, we have edited the video footage obtained into a short videotape (running time approximately 12 minutes) which also has some slow motion segments which amplify more clearly the points made with reference to the still photos presented herein. The videotape is available for at-cost purchase from the authors.

As noted, two basic types of ball-powder-ball events—impacts and rolling/sliding—are common to the attritor. Our observations show that the relative occurrence of these different types of collisions depends on location within the device. The regions are effectively discussed in terms of three surfaces, r-θ, r-z, and z-θ, as shown in Figure 3. These surfaces describe the possible geometrical translations and rotations of the grinding media under the constraints provided by the attritor canister. Understanding the natural flow of the grinding media along these surfaces provided us with the means of ascertaining velocity gradients within the mill.

IV. RESULTS

In the following sections, observations made from the video recording are synopsized. These are supplemented by results from ancillary experiments. In addition, we present some qualitative analysis of attritor dynamics made possible *via* frame-by-frame scrutiny of the film, along with observations made with stroboscopic illumination. We first describe the dynamics of ball motion in an attritor absent a powder charge. This is followed by a similar description made with a powder charge present in the attritor.

A. *The Geometry of the Ball Array*

When grinding balls are placed in a canister, they assume a random dense-packed array. On a size scale of the order of several balls in two dimensions, the array is a mixture of close packed and square packing. During attritor operation at 50 rpm, this "composite" array is distorted (Figure 4(a)). At higher rotational speeds (250 rpm and greater), the balls assume a close-packed

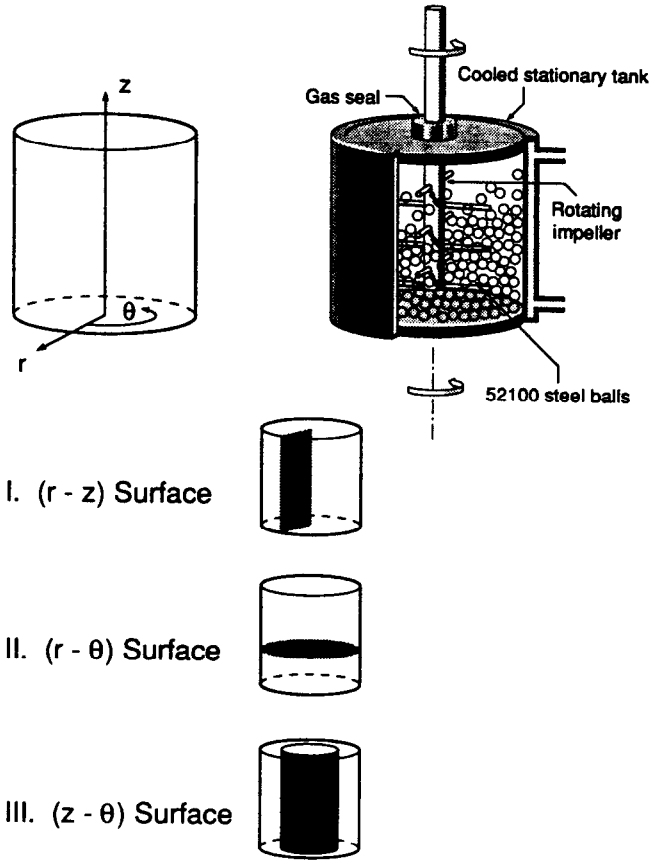

Fig. 3—Three reference surfaces used to describe media motion: an *r-z* surface defines motion in a vertical plane extending from the impeller arm to the canister wall; an *r-θ* surface does the same in a horizontal plane; whereas a *z-θ* surface determines relative rotational motion.

hexagonal array within *z-θ* planes in regions of the attritor outside of the impeller core (Figure 4(b)). Vacancies are found in this lattice-like arrangement, and they provide a mechanism for both impact events and ball circulation within the mill. When a ball makes a radial transit from an inner layer, it either collides with a ball in the next layer out or with the mill wall. Alternatively, a ball can drop into a vacancy from a layer displaced vertically by one ball diameter. Both kinds of transit provide a means for ball circulation. Vacancies appear to be dynamically created; a mechanism for doing this is shown in Figure 5. The illustration depicts a unit cell of the array; the schematic on the left side of the figure shows the "average" unit cell, whereas that on the right side indicates that the near-neighbor spacing varies during mill operation. When the spacing between adjacent ball surfaces exceeds approximately one ball diameter, the resulting "dynamic" vacancy can be annihilated by either of the ball transits described above. (There are probabilistic considerations, of course. Some vacancies self-annihilate prior to annihilation effected by a ball transit.)

Viewing the videotape provides little appreciation of the rate of ball migration accomplished in the above manner. In fact, due to the high film speed, such interchanges appear to occur infrequently. This is not so. We investigated the diffusion or interchange of balls on the

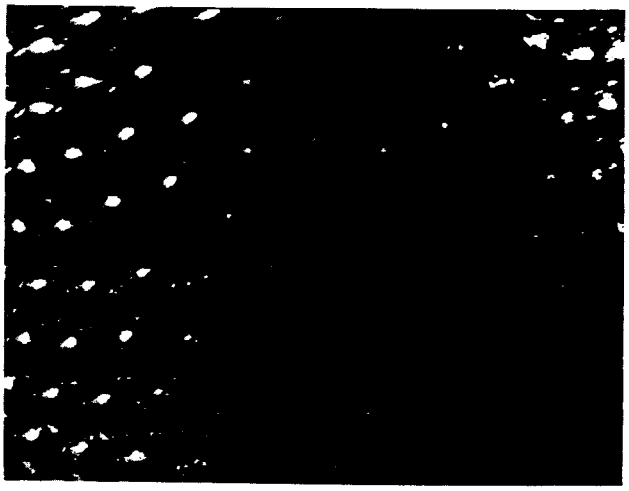

(*a*)

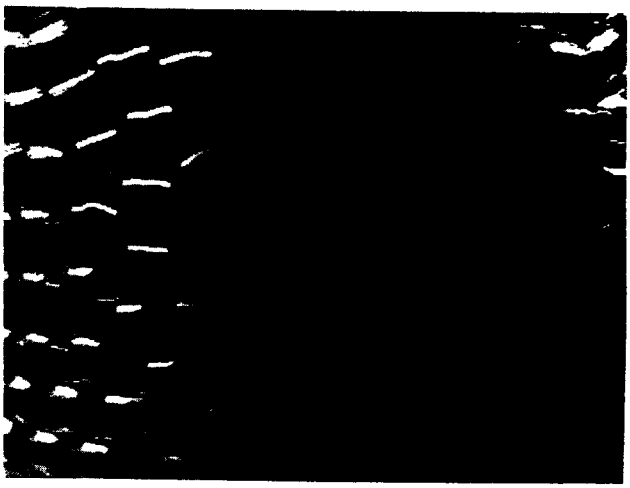

(*b*)

Fig. 4—Still photos of ball motion viewed from the attritor side. (*a*) Rotational velocity = 50 rpm. The center of the picture approximately corresponds to the instantaneous (projected) position of the impeller arm. The ball array is most distorted here; some vacancies can be seen. (*b*) Rotational velocity = 250 rpm. The close-packed ball array characteristic of high rotational velocities is apparent at the bottom center and right-hand sides of the photo. Vacancies can be seen near the center of the photo.

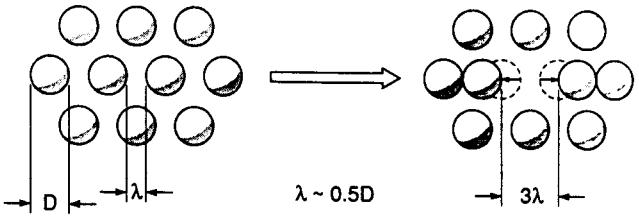

Fig. 5—Schematic of dynamic vacancy creation mechanism. The close-packed ball array is illustrated on the left. While the array is close packed, the ball surfaces do not touch in operation; they are on average separated by a distance, λ, which is on the order of the ball radius. The arrangement is dynamic, and during operation, the surface-to-surface separation distance varies. When it becomes large enough (*e.g.*, 3λ as shown in the right), a vacancy can be considered formed. The vacancy can be annihilated by a ball falling vertically into the site or by a ball being displaced by centripetal force from a layer displaced one ball diameter toward the attritor core.

outermost ball layer by placing colored balls in the outermost ring of the attritor prior to operation. These balls were displaced to interior positions within a maximum time of 30 seconds of operation, with the longer times in this range being required for interchange at higher rotational velocities. The centripetal force arising from mill rotation may be considered analogous to an activation energy. At higher velocities, interchange takes place by a "vacancy" mechanism, while at low velocities, the "diffusion" mechanism is "viscous" flow within the more disordered ball array characteristic of low rotational velocities.

B. *Velocity Gradients in r-θ Planes*

We were able to directly observe ball motion at the attritor top and bottom. A still from the attritor top for a rotational velocity of 50 rpm is shown in Figure 6(a). Even at this low speed, impeller arm agitation is sufficient to force a significant fraction of the balls away from the attritor core. The voided region is approximately cone shaped. Accompanying this displacement, we find that balls nearest the canister wall stack to a height greater than those in the interior. Increasing attritor rotational velocity exaggerates these effects; *i.e.*, the cone volume is increased, and thus, fewer balls are located within the core and more on the periphery. Thus, even though higher rotational speeds provide greater impact velocities in the attritor core and presumably a higher frequency of impacts, there are fewer balls available to partake in such events at such speeds. This suggests that while the "action" needed for MA may well be most effective in the core, the portion of powder which experiences this action may be limited.

A still photo, taken from the top of the attritor operating at 250 rpm, is shown in Figure 6(b). At this rotational velocity, the balls are moving sufficiently rapidly that individual motion of a specific ball cannot be resolved. This motion, however, is revealed by "streaklines"; the lengths of these provide a measure of the distance traveled by a ball within the time duration of one film frame. Inside the attritor core, streakline lengths are about the same, indicating balls in the core all move with approximately the same velocity at higher rpm.

We measured angular velocities of the balls as a function of radial position in the attritor. This was made possible with a frame-by-frame advance of the video recording. Results of such measurements, taken at the top of the mill for a rotational velocity of 50 rpm, are given in Figure 7. Angular velocities approach, but do not equal, zero along the attritor wall, and the angular velocity increases monotonically from the canister wall to the tips of the impeller arms. The gradient in angular velocity provides for what we call z-θ shear. This type of shear corresponds essentially to rolling/sliding events. Relative sliding is greatest for layers removed from the core. The high ball velocities characteristic of operation at a rotational velocity of 250 rpm precluded quantitative assessment of relative rotational velocities for this operating condition. However, stroboscopic observations indicated that the velocity in the core is approximately constant, in agreement with statements made previously with respect to streakline lengths.

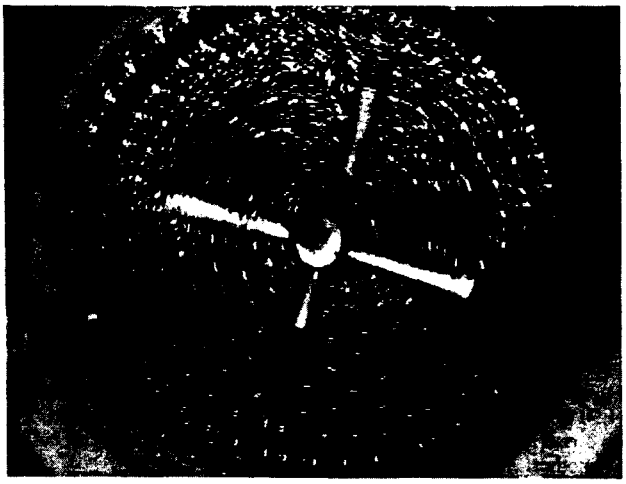

(*a*)

(*b*)

Fig. 6—View of the attritor top when operating at (*a*) 50 rpm and (*b*) 250 rpm. The centripetal force displaces balls toward the canister wall; the effect is greater the higher the rotational velocity. A cone-shaped void is formed concurrently in the core; the voided volume increases with rotational velocity. "Streaklines" are a characteristic of the still taken at 250 rpm. The line lengths represent the distance traveled by a ball within the time duration of one film frame. As the line lengths are approximately the same, the balls move at about the same velocity at the mill top at the higher rpm. This is not so at low rotational speeds.

Ball motion is more constrained at the mill bottom, as shown in the still photos of Figures 8(a) and (b). The constrained motion presumably arises, in part, because the bottom of the impeller shaft is located two ball layers above the canister bottom and, in part, because of the restraint on ball motion provided by the weight of the balls in the attritor. In fact, the clarity with which individual balls can be identified in Figure 8(a) indicates that for a rotational velocity of 50 rpm, little energy is transmitted to the bottom layer of the balls, and they consequently move slowly. Indeed, the velocities of the peripheral rings of balls approach zero and are also low in other locations. This is one reason why a "dead" zone is characteristic of an attritor.

Rotational velocities were measured at the mill bottom

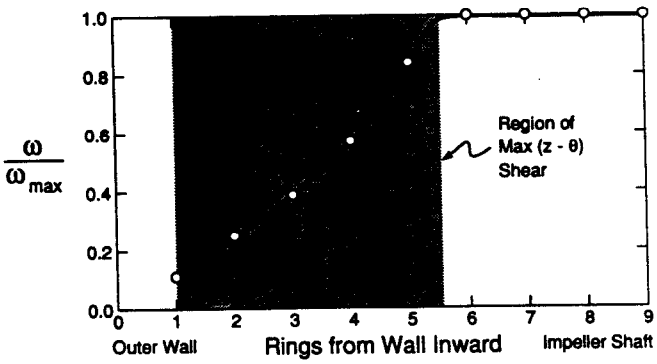

Fig. 7—Rotational velocities at the mill top for an attritor operating at 50 rpm. Velocity gradients are found outside the core region. These give rise to sliding (rolling) displacements (z-θ shear), one ball ring to another.

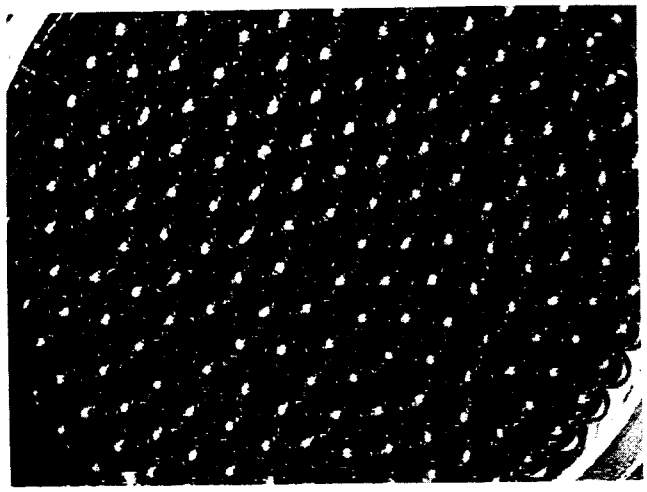

(*a*)

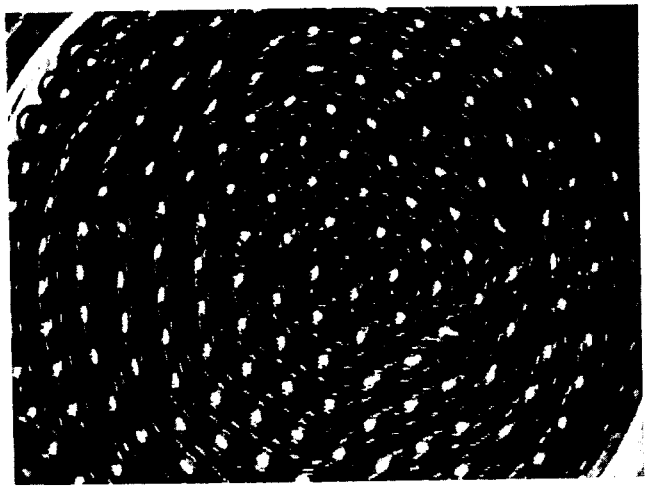

(*b*)

Fig. 8—Still photos of the attritor bottom for operation at (*a*) 50 rpm and (*b*) 250 rpm. Ball motion is constrained here because of the weight of the balls above this layer and because the bottom of the impeller shaft is located several ball diameters above the tank bottom. Greater ball motion is evident at 250 rpm. Some "vacancies" can be seen, and the ball array pulsates between a hexagonal and pentagonal array (see Fig. 10).

for a rotational velocity of 250 rpm (Figure 9). Rotational velocities are greatest near the impeller arm tips and decrease as the canister wall is approached, suggesting the possibility of a turgid or dead zone in this case also. Although the dead zone is discussed in more detail later, we note here that the mill bottom is not completely quiescent. For example, at rotational velocities of 250 rpm, we noticed that near the attritor core, the balls pulsate between a pentagonal and hexagonal array, as illustrated in Figure 10. During the pulsations, balls are thought more capable of interchange between the bottom ball layer and the layer immediately above this one. This interchange mechanism is roughly the analog of the vacancy mechanism described previously and which pertained to radial interchange of the grinding media. Interchanges at the mill bottom might facilitate powder transport from this region. Extensive segregation of powder to the mill bottom is characteristic of MA in an attritor, as is discussed in Section V.

C. *Velocity Gradients in z-θ Planes*

Using the single frame advance method, we made fairly accurate measurements of ball velocities along the mill walls. Results are shown in Figure 11 for the two rotational velocities investigated. In analogy with the radial velocity gradients (which give rise to z-θ shear), vertical velocity gradients cause what we term r-θ shear. The measured velocity profile at 50 rpm is in qualitative accord with the ideas of Lavarev *et al.*,[24] who suggested that "driving forces" are transmitted through narrow regions extending out from the impeller paddles. The

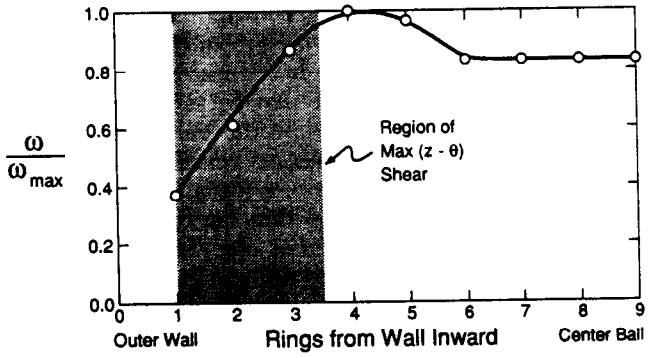

Fig. 9—Rotational velocities at the mill bottom for attritor operation at 250 rpm. Velocity gradients are observed near the canister wall. These are also manifestations of z-θ shear.

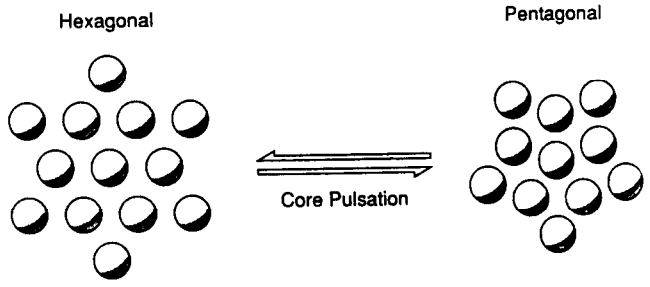

Fig. 10—"Pulsations" in ball packing are noticed on the mill bottom in the region near the attritor core. The ball array alternates between a hexagonal (left) and a pentagonal (right) one.

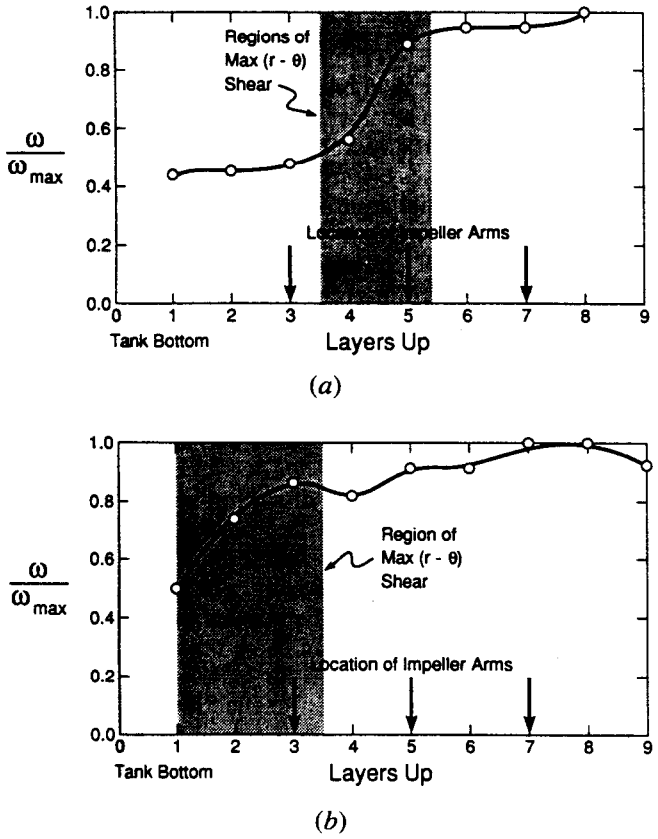

Fig. 11 — Vertical velocity gradients along the mill side for operation at (*a*) 50 rpm and (*b*) 250 rpm. At the low rpm, velocities are either "low" (near the bottom) or "high" (near the top). The transition in velocity is associated with the vertical position of an impeller arm. The velocity gradient gives rise to relative ball sliding/rolling (r-θ shear). At the higher rpm, the transition from low-to-high velocity, and thus, the greatest r-θ shear, is found near the mill bottom (perturbations in the high-velocity region are associated with impeller arm positions).

impeller arms (particularly the one located five layers up) destroy the periodic array as they pass, resulting in the stepped velocity profile shown. However, at 250 rpm, there is minimal disturbance of the close-packed array, leading to a smoother velocity profile.

Our observations on milling dynamics are summarized as follows. Rotational velocity gradients exist along both radial and vertical directions in an attritor. These give rise to sliding/rolling events, and such occurrences are far more common than are direct impacts, which occur most frequently in the attritor core. However, direct impacts do occur outside of the core, and even though relatively few in number, they take place at a rapid rate when measured in "real time." We believe impact events are more effective than rolling/sliding ones for powder deformation, fracture, and coalescence, and offer substantiation of this in Section VI.

V. POWDER MIGRATION AND SEGREGATION

When introduced into an operating mill, powder segregates rapidly to the device bottom, as shown in

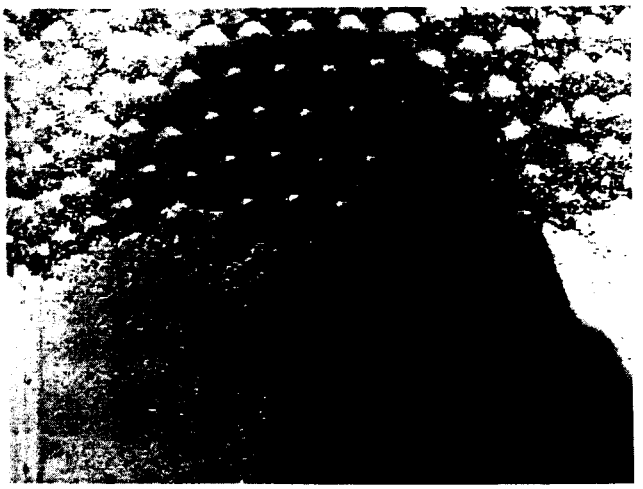

Fig. 12 — Still photo taken from the tank side illustrating powder segregation during operation at 50 rpm (the degree of segregation is essentially the same for operation at 250 rpm). The tank bottom corresponds to the picture bottom. Thus, powder is located primarily in the lowermost several ball layers. Note, though, the powder coating on the balls in other locations.

Figure 12. At any time, a disproportionate fraction of the powder charge resides along or near the mill bottom. Conversely, only a small fraction of the powder is located within the attritor core. The apportionment of powder in the various sectors of the mill is also evidenced by the distribution of powder which has been cold welded to the impeller arms and to the tank. There is only a slight buildup of mill debris on the upper impeller arms. In distinction, the bottom arms are fairly heavily coated with powder. This is a reflection of gravity-induced powder segregation. Powder caking was also observed along the canister walls, as shown schematically in Figure 13. Regions of little or no debris buildup are found at the center and outside edges of the mill bottom, indicating little mill activity takes place in these regions. Light caking observed between these regions correlates with the maximum z-θ shear (*cf.* Figure 9). Little or no caking is observed along the side walls of the attritor bottom for a height upward of about two to three ball diameters. This region near the bottom periphery of the canister, which contains a significant fraction of the powder charge, is the attritor dead zone. Heavy caking is found along the canister wall immediately above the dead zone. A thinner coating is found along the upper portions of the wall. This coating is fairly uniform in thickness and extends up to the maximum height attained by the rotating grinding media.

Based on these observations, we have divided the attritor into several volumes, as indicated in Figure 14. To a first approximation, the attritor can be considered composed of the core region (region 2, where the impeller arms are situated) and a region outside of the core. Within the core, direct impacts are prevalent; outside this region, they occur with less frequency and energy, and diffusion of the balls takes place at a much lesser rate (*e.g.*, as in region 1, limited diffusion). The inactive volume, though, can be subdivided into several regions, including ones of maximum z-θ shear (region 3), r-θ shear

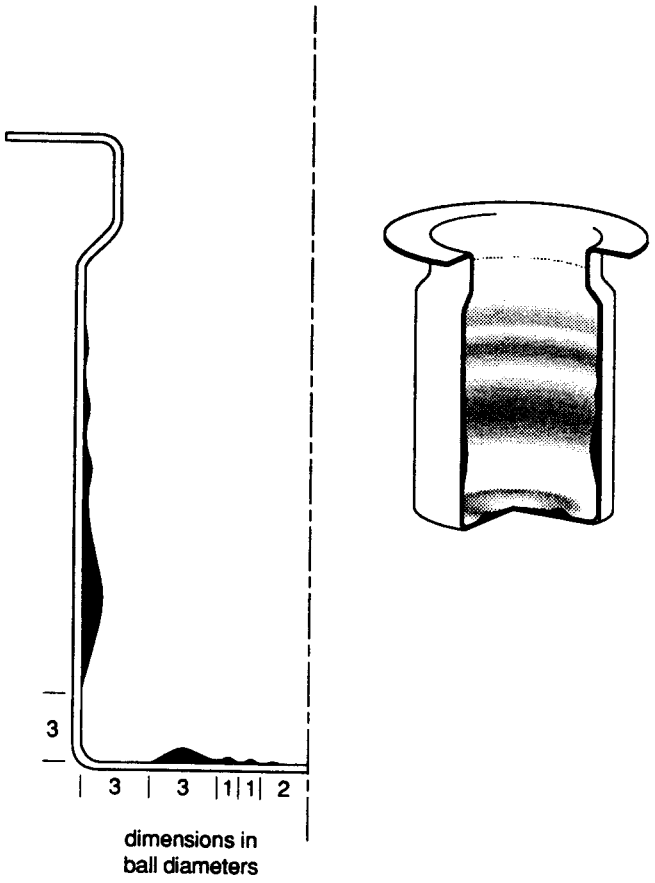

Fig. 13—Powder caking during attritor operation at 250 rpm. The shaded areas of the cut-away sketch of the tank (on right) indicate areas where caking is found. The vertical section on the left semi-quantitatively indicates the extent of powder caking. No caking is observed in the attritor dead zone (the bottom edge of the attritor). Light caking on the mill bottom correlates with the region of maximum z-θ shear. Heavy caking is observed on the wall above the dead zone, and a thinner powder coating is found along the upper portions of the wall.

(region 4), as well as a dead zone (region 5, the zone of limited ball and powder migration). A preponderance of rolling/sliding events takes place in the zones of maximum shear. Their locations (and relative volumes) are only indicated approximately in Figure 14, as they depend on rotational velocity (*cf.* Figures 7, 9, and 11).

We have also constructed a schematic mill powder migration pattern (Figure 15). Powder rapidly migrates downward through the mill as a result of gravity. Balls (and powder) circulate radially within the mill but also can be removed from the mill bottom by virtue of ball motion, described previously. The balls (and powder) vacated in this way are replaced (replenished) by gravity-induced flow as well as radial displacements at the mill bottom. Powder and balls which move into the impeller core are subsequently displaced toward the canister wall. The pattern sketched suggests that powder does flow, albeit sluggishly, through the whole of the attritor. The slow rate at which it does, though, accounts, in part, for the inefficiency of the attritor as an MA device. Additional ideas relative to attritor efficiency are provided in the following section.

VI. ADDITIONAL REMARKS ON ATTRITOR EFFICIENCY

We have shown that both rolling/sliding and direct impacts occur in an attritor. In preceding discussions, we have postulated that direct impacts are more effective for causing the processes eventuating in MA. In this section, we present additional arguments to support this premise.

Viewed in slow motion, rolling is seen as a series of discrete, low-speed collisions rather than a continuous process. So while rolling does occur in the mill volume outside the core, the pertinent question is the relative efficacy of these collisions. In addition, since rolling on the tank bottom differs from that on the mill sides in terms of the forces and velocities characteristic of each, rolling in the different mill regions will have correspondingly different efficiencies.

We discuss the efficiency of rolling in different zones and then compare it to the efficiency of a direct impact event. We consider first the tank bottom, with the purpose of determining whether rolling at this location can effect plastic deformation of the powder there. The weight of the balls provides a normal force on this powder; the force is on the order of 0.1 N for balls of the type common to a laboratory attritor. Plastic flow will occur if this load is supported over a sufficiently small area. The elastic limit of the powder is exceeded if the force exceeds the powder hardness times the area of contact; *i.e.*, this force is given by

$$F_{ER} = H_v \pi a^2 \qquad [1]$$

where H_v is the Vickers hardness and a the contact radius. A soft powder might have a hardness on the order of 150 MPa; this gives a required contact radius of approximately 15 μm. In light of the amount of powder on the mill bottom and previous calculations of contact area,[18] it seems unreasonable to expect such a small quantity of powder trapped under a ball. However, the aforementioned caking indicates that plastic deformation does occur in certain portions of the mill bottom. We conclude this must be the result of impact events from balls one layer up striking balls on the bottom layer.

The stresses on the tank wall originate from centripetal acceleration of the stirred media. The rolling "force" can be estimated as

$$P = m\omega^2 R \qquad [2]$$

where m is the mass of balls in a "line" from the center of the tank to the wall, ω the rotational frequency of the balls, and R the tank radius. For a mill rotational velocity of 500 rpm, the value of this force is calculated as 0.05 N, even less than the value calculated for the mill bottom. Thus, it is even more unlikely that rolling alone produces plastic deformation on the canister wall.

If we then suppose that impacts are responsible for powder plastic deformation, the pertinent parameters are the impact velocity and frequency, as well as the variation of these parameters within the attritor zones. Based on the experimental results of this study, ball velocities can be determined from rotational frequencies and for different radial positions in an attritor. A failing of this approach is that we are restricted to measurements made on balls nearest the mill surface. In addition, it is likely

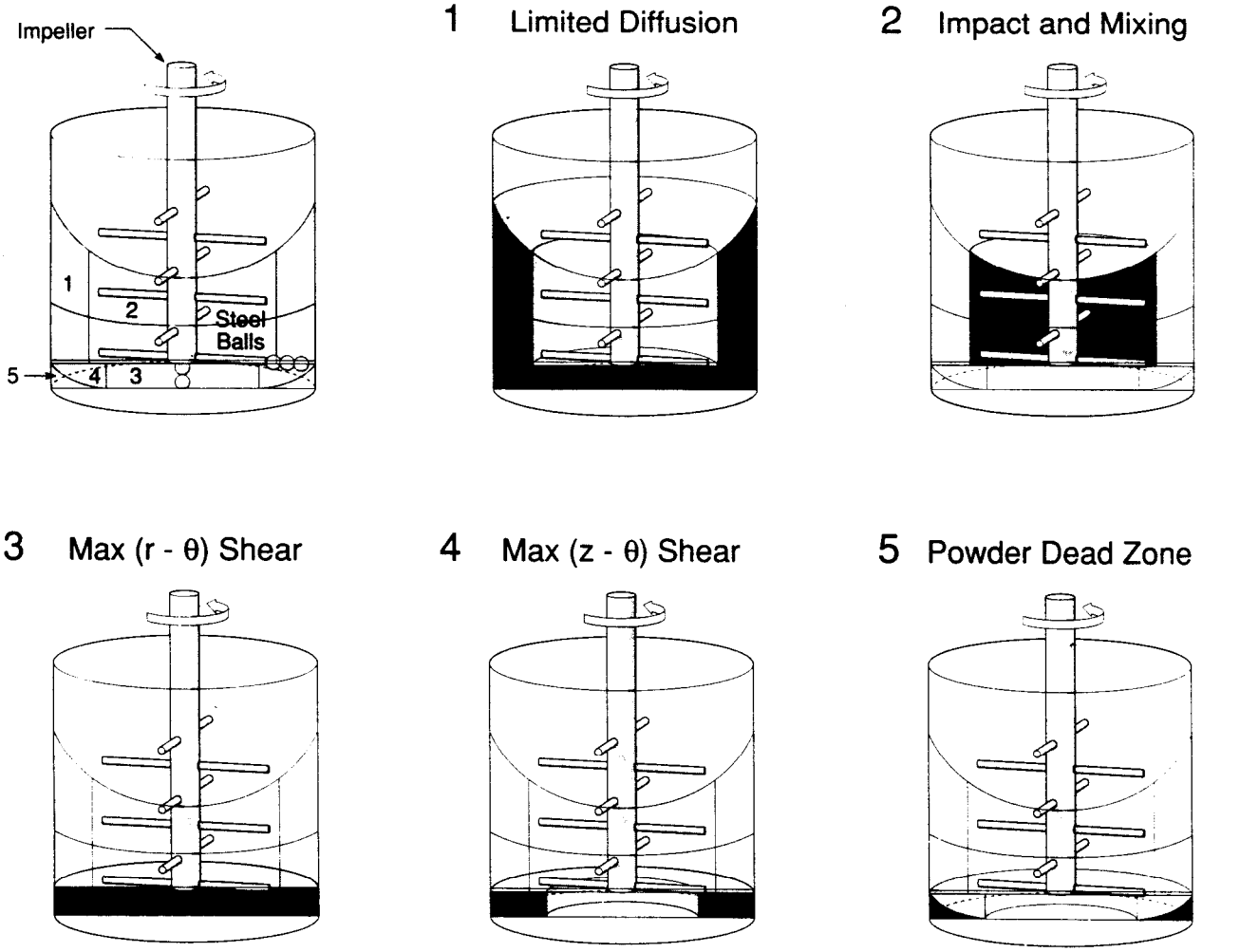

Fig. 14—Regions of the attritor manifesting differing milling actions. The mill can be first divided into the core (region 2, where direct impacts and vigorous mixing take place) and the remainder of the attritor (where these events are much less pronounced). The latter region can be subdivided. The dead zone (region 5, near the bottom edge of the attritor) is quiescent. Regions of maximum r-θ shear (region 3) occur along r-θ planes; regions of maximum z-θ shear are located along the outer wall and extend several ball layers up. Limited ball diffusion is found primarily in the upper portion of the mill lying outside the attritor core (region 1). The precise locations of the several regions and their relative extent depend upon mill rotational speed.

that the velocity of an impact is substantially greater than that of a ring or layer of balls.

As an alternative to such indirect measurements, we took Pb balls of the same size as the steel balls and placed the Pb ones in strategic locations within the tank. The Pb balls were sufficiently low in number that collisions between them did not occur. The idea is that a Pb ball would reasonably mimic a powder coated one but would maintain a permanent artifact in the form of an indentation for each impact. These indentations could then be counted to determine impact frequency. Assuming the kinetic energy of a steel ball is expended in plastic deformation of the Pb one, the size of the indentation can be used to determine a relative impact velocity *via*[28] (ignoring factors of order unity)

$$v = \left(\frac{a}{R_b}\right)^2 \left(\frac{H_v}{\rho}\right)^{1/2} \qquad [3]$$

where a is the indentation radius, R_b the ball radius, H_v the hardness of the lead balls, and ρ the density of the steel balls. Experiments of this nature were carried out for very short milling times (on the order of slightly greater than 1 second) so that individual indentations could be counted and their areas approximately determined by viewing them with an optical microscope attached to a microhardness indenter. [We caution that the (necessarily) crude methodology results in data subject to considerable scatter.] Results of this study are shown in Table I, which summarizes collision frequencies and relative impact velocities in the several attritor zones (the zone locations are noted in Figures 13 and 14). The regions where powder caking was observed are characterized by relatively high frequencies and velocities. In contrast, the powder dead zones (where no caking was observed) are essentially devoid of direct impacts.

VII. IMPROVED ATTRITOR DESIGN

Most MA devices, including an attritor, are typically inefficient in that only a small fraction of the expended energy results in the powder deformation, welding, and

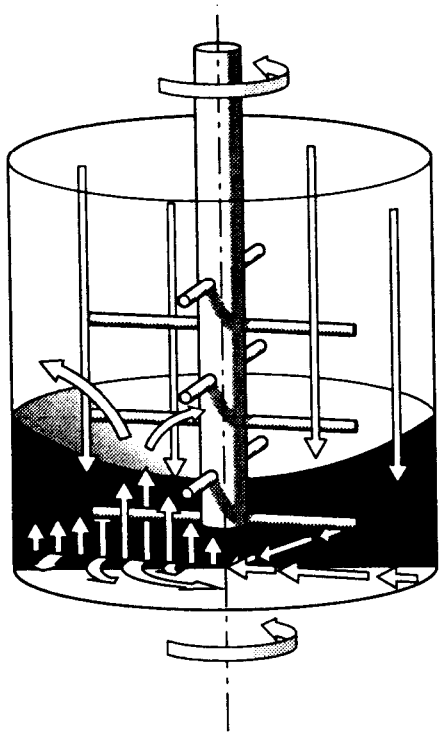

Fig. 15—Schematic of powder circulation in an operating attritor. Powder segregates vertically due to gravity. It also is displaced rotationally as a result of impeller arm motion. Powder (and balls) can be displaced upward by interchanges between balls at the mill bottom and those above it. When such a displacement moves a ball (and its associated powder) into the attritor core, it is subsequently displaced toward the canister wall by the vacancy mechanism. Balls (and powder) then resegregate to the mill bottom.

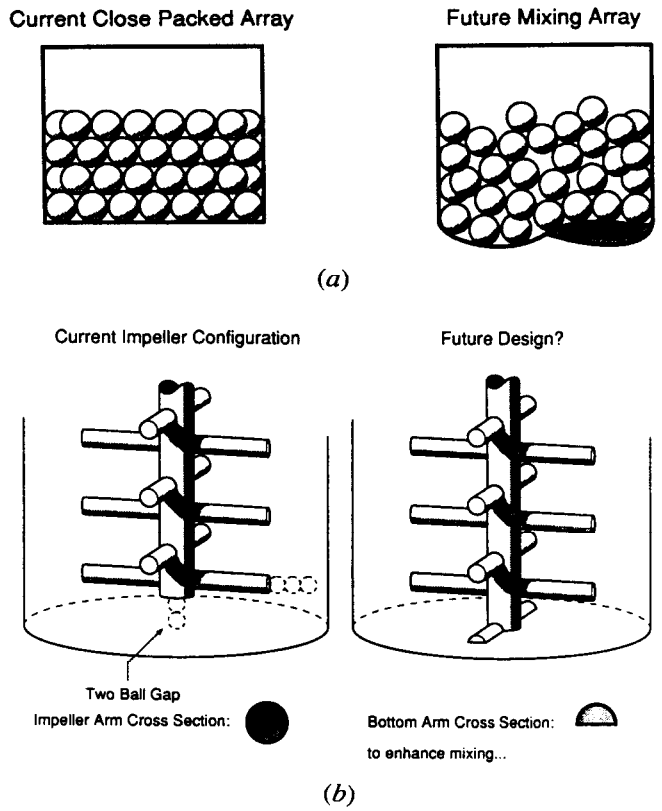

Fig. 16—Suggestions for improved attritor design: (*a*) using a contoured, rather than flat, mill bottom might facilitate steering balls and powder into the more active mill regions and (*b*) using an additional half impeller arm located near the mill bottom might displace balls up from the mill bottom and into the more active regions.

fracture requisite for MA. Attritor efficiency is further limited by virtue of its geometrical characteristics and dynamics, as described in this article. Elimination of the dead zone and a means for facilitating powder circulation within the mill could reduce the process time for an attritor. On these premises, we suggest three approaches which might lead to improved attritor efficiency.

The first focuses on the geometrical characteristics of the grinding media. We have shown that milling with balls having the same diameter results in a close-packed ball array in the attritor volume outside of the core. Such an array results in a predominance of rolling, rather than impact, events. Use of balls with two (or more) different diameters would presumably prevent the close-packed array from forming, with an attendant increase in mill agitation. The result could be more direct impact events (considered more efficient for effecting MA) and a lesser relative number of rolling/sliding ones. The other approaches could facilitate powder removal from the dead zone and/or reduction of this zone's volume. The bottom of the attritor container could be contoured in such a way as to steer balls and powder up into the more active mill regions (Figure 16(a)). An additional arm could be placed on the attritor shaft, as indicated in Figure 16(b); this (the lowest) arm could be machined into a wedge—as opposed to the current round—shape.

Table I. Impact Frequency and Velocity in Different Locations of an Attritor

Location and Impeller Frequency (rpm)		Frequency (s^{-1})	Velocity (m/s)
Limited diffusion, 4 to 6 layers up	(250)	1.56	0.2
	(500)	2.58	0.7
Impact and mixing	(250)	0.59	0.3
	(500)	2.35	0.9
Bottom near middle	(250)	0.0	0.0
	(500)	0.27	0.1
Bottom, high shear zone	(250)	0.89	0.2
	(500)	1.06	0.3
Powder dead zone	(250)	0.0	0.0
	(500)	0.0	0.0

This would force balls up from the mill bottom and into the more active regions. Other balls will fall to fill the volume vacated by balls circulated in this way, thus creating a localized convection of powder and grinding media.

VIII. SUMMARY

A high-speed cinematographic study of the dynamics of an attritor has been conducted. The resultant video, along with observations taken from it and ancillary measurements, allows us to define several regions of activity within an attritor. The region outside the volume containing the attritor arms is relatively inactive. In fact, a dead zone, containing a disproportionately high volume fraction of powder, exists at the periphery of the mill canister bottom. However, some regions of the attritor outside the volume containing the arms are characterized by ball velocity gradients which provide a mechanism for mechanical action by ball sliding and a means for powder circulation within the attritor. Additional experiments indicate that direct impacts, rather than rolling/sliding events, are primarily responsible for the mechanisms effecting MA. The results of this investigation provide some suggestions for more efficient attritor design.

ACKNOWLEDGMENTS

The authors are grateful to Mr. William Edwards for designing and constructing the model attritor. Thanks are due to W.S. Arbogast and C.L. Tate for assisting in the production of the video presentation. Discussions with Dr. H.N.G. Wadley are appreciated. DARPA/NASA supported the efforts of RWR and DM. The Army Research Office supported those of THC.

REFERENCES

1. John S. Benjamin: *Metall. Trans.*, 1970, vol. 1, pp. 2943-51.
2. J.S. Benjamin and T.E. Volin: *Metall. Trans.*, 1974, vol. 5, pp. 1929-34.
3. P.S. Gilman and J.S. Benjamin: *Ann. Rev. Mater. Sci.*, 1983, vol. 13, pp. 279-300.
4. J.S. Benjamin, T.E. Volin, and J.H. Weber: *High Temp.–High Pressures*, 1974, vol. 6, pp. 443-46.
5. R.C. Benn, J.S. Benjamin, and C.M. Austin: *High Temperature Alloys: Theory and Design*, J.O. Steigler, ed., TMS-AIME, Warrendale, PA, 1984, pp. 419-49.
6. P.S. Gilman and W.D. Nix: *Metall. Trans. A*, 1981, vol. 12A, pp. 813-24.
7. J.H. Weber: in *Solid State Powder Processing*, A.H. Clauer and J.J. deBarbadillo, eds., TMS-AIME, Warrendale, PA, 1990, pp. 227-39.
8. M.S. Kim and C.C. Koch: *J. Appl. Phys.*, 1987, vol. 62, pp. 3450-57.
9. M.A. Morris and D.G. Morris: *Solid State Powder Processing*, A.H. Clauer and J.J. deBarbadillo, eds., TMS-AIME, Warrendale, PA, 1990, pp. 299-314.
10. I.J. Lin and S. Nadiv: *Mater. Sci. Eng.*, 1979, vol. 39, pp. 193-209.
11. T. Kosmac and T.H. Courtney: *J. Mater. Res.*, 1992, vol. 7, pp. 1519-25.
12. S.H. Han, K.A. Gschneider, Jr., and B.J. Beaudry: *Scripta Metall Mater.*, 1991, vol. 25, pp. 295-98.
13. R.B. Schwartz, R.R. Petrich, and C.K. Saw: *J. Non-Cryst. Solids*, 1985, vol. 76, pp. 281-302.
14. E. Hellstern, H.J. Fecht, Z. Fu, and W.L. Johnson: *J. Appl. Phys.*, 1989, vol. 65, pp. 305-10.
15. E. Gaffet and M. Harmelin: *J. Less-Common Met.*, 1990, vol. 157, pp. 201-22.
16. C.C. Koch, O.B. Cavin, C.G. McKamey, and J.O. Scarbrough: *Appl. Phys. Lett.*, 1983, vol. 43, pp. 1017-19.
17. G. Wang, D. Zhang, H. Chen, B. Lin, W. Wang, and Y. Dong: *Phys. Lett.*, 1991, vol. A155, pp. 57-60.
18. D.R. Maurice and T.H. Courtney: *Metall. Trans. A*, 1990, vol. 21A, pp. 289-303.
19. T.H. Courtney and D.R. Maurice: in *Solid State Powder Processing*, A.H. Clauer and J.J. deBarbadillo, eds., TMS-AIME, Warrendale, PA, 1990, pp. 3-19.
20. B.J.M. Aikin, T.H. Courtney, and D.R. Maurice: *Mater. Sci. Eng.*, 1991, vol. 147A, pp. 229-37.
21. R.M. Davis, B. McDermott, and C.C. Koch: *Metall. Trans. A*, 1988, vol. 19A, pp. 2867-74.
22. R.B. Schwartz and C.C. Koch: *Appl. Phys. Lett.*, 1990, vol. 49, pp. 146-48.
23. G. Martin and E. Gaffet: *J. Phys. France (Coll.)*, 1990, vol. 51, pp. C4-15.
24. A.S. Lavarev, A.A. Kolesnikov, and V.A. Koral: *Sov. Powder Metall. Met. Ceram.*, 1987, vol. 25, pp. 613-17.
25. R. Goodson, F. Larson, and L. Sheehan: *Int. J. Refract. Hard Met.*, 1985, vol. 4, pp. 70-76.
26. H.E. Rose and R.M.E. Sullivan: *A Treatise on the Internal Mechanics of Ball, Tube and Rod Mills*, Chemical Publishing Company, New York, NY, 1958.
27. H. Kimura, M. Kimura, and F. Takada: *J. Less-Common Met.*, 1988, vol. 140, pp. 113-18.
28. D. Maurice and T.H. Courtney: University of Virginia, Charlottesville, VA, and Michigan Technological University, Houghton, MI, unpublished research, 1992.